Journal of ELECTRONIC MATERIALS, Vol. 45, No. 4, 2016
DOI: 10.1007/s11664-016-4359-y
© 2016 The Minerals, Metals & Materials Society

CrossMark

High-Resistivity Semi-insulating AlSb on GaAs Substrates Grown by Molecular Beam Epitaxy

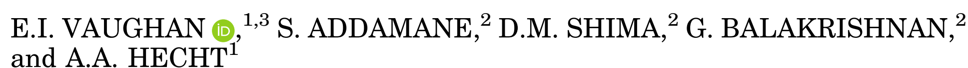
E.I. VAUGHAN,[1,3] S. ADDAMANE,[2] D.M. SHIMA,[2] G. BALAKRISHNAN,[2] and A.A. HECHT[1]

1.—Department of Nuclear Engineering, University of New Mexico, MSC01 1120, 1 University of New Mexico, Albuquerque, NM 87131, USA. 2.—Center for High Technology Materials, University of New Mexico, Albuquerque, NM 87131, USA. 3.—e-mail: ehusher@unm.edu

Thin-film structures containing AlSb were grown using solid-source molecular beam epitaxy and characterized for material quality, carrier transport optimization, and room-temperature radiation detection response. Few surface defects were observed, including screw dislocations resulting from shear strain between lattice-mismatched layers. Strain was also indicated by broadening of the AlSb peak in x-ray diffraction measurements. Threading dislocations and interfacial misfit dislocations were seen with transmission electron microscopy imaging. Doping of the AlSb layer was introduced during growth using GaTe and Be to determine the effect on Hall transport properties. Hall mobility and resistivity were largest for undoped AlSb samples, at 3000 cm^2/V s and 10^6 Ω cm, respectively, and increased doping levels progressively degraded these values. To test for radiation response, *p*-type/intrinsic/*n*-type (PIN) diode structures were grown using undoped AlSb on *n*-GaAs substrates, with *p*-GaSb cap layers to protect the AlSb from oxidation. Alpha-particle radiation detection was achieved and spectra were produced for ^{241}Am, ^{252}Cf, and ^{239}Pu sources. Reducing the detector surface area increased the pulse height observed, as expected based on voltage–capacitance relationships for diodes.

Key words: High resistivity, AlSb, MBE, room-temperature radiation detectors, thin films, Hall measurements

INTRODUCTION

AlSb remains a material of interest for potential applications in room-temperature radiation detection due to its large bandgap of 1.62 eV at 300 K and the high atomic number of Sb. Efforts to further characterize AlSb have been met with challenges on account of the highly reactive nature of Al with oxygen, and Sb and molten AlSb being extremely volatile, reacting with nearly all crucible materials. AlSb also oxidizes rapidly in air, further complicating handling. While AlSb is theorized[1] to have high resistivity and high and dual carrier mobility, these properties have been inconsistently reported[1–5] due to difficulties in bulk growth of high-quality AlSb material. Molecular beam epitaxy (MBE) is routinely used to fabricate devices containing AlSb layers as insulating buffers[4] and in quantum well structures,[6] among other applications. We have used this same method to grow very high-quality, potentially detector-grade AlSb material.

For uniform detector response, large and symmetric mobility and lifetime properties are desired. Semiconductor detectors fabricated from materials with nonsymmetric properties suffer from reduced resolution due to the location-dependent response of radiation interactions. This is a well-known disadvantage for CdZnTe detectors because of poor hole transport. Additional transport properties used to evaluate materials for semiconductor device applications include resistivity, mobility, and carrier concentration. These parameters are very sensitive

(Received August 22, 2015; accepted January 16, 2016; published online February 11, 2016)

to growth conditions, defects, and impurity levels, and can vary greatly as a result. Most AlSb characterization reports seen in literature[1–3] are representative of material grown by bulk methods, where oxidation and reactivity with crucibles introduce large concentrations of defects and impurities. The best reported bulk AlSb values for resistivity, mobility, and carrier concentration are 8×10^5 Ω cm,[1] 450 cm^2/V s (holes),[2] and $< 10^{12}$ cm^{-3},[3] respectively. Theory[1] predicts resistivity of 10^{12} Ω cm and electron mobility of 1200 cm^2/V s for pure AlSb. It should also be noted that theoretical calculations performed by Erhart et al.[3] predict weakly n-type conductivity for pure AlSb, whereas experimental results for bulk-grown AlSb[3,7,8] all exhibited p-type characteristics. This was attributed to impurities and defects introduced during growth.

As epitaxial methods are routinely used to grow AlSb as inactive layers in heterostructures, transport properties are not often measured or reported, although the semi-insulating nature of MBE-grown AlSb has been accepted[4] for several decades. Ultrahigh-vacuum (UHV) MBE growth eliminates many of the contaminants that are problematic for bulk growth, and also enables precise control of layer thickness and dopant concentration.

EXPERIMENTAL PROCEDURES

Material Fabrication and Structure Design

Heterostructures composed of GaAs, GaSb, and AlSb were grown using a twin VG V80 MBE reactor with valved As and Sb crackers and VEECO's SUMO™ effusion cells for In, Ga, and Al. The Al and Sb used for this work had 7 N purity.

Samples composed of one of two structures were grown on GaAs substrates. For material quality and doping study purposes, the first structure contained 3 μm of AlSb, undoped and with different levels of n- and p-doping, on semi-insulating (SI) GaAs with 10 nm GaAs as an oxygen-protective cap layer. The second structure, used for diode characterization and radiation response measurements, consisted of 5 μm undoped AlSb on n-type GaAs substrates with 5 nm p-type GaSb as the oxygen-protective cap layer. Planar ohmic contacts were applied to the top and bottom surfaces of the diode structure.

Characterization Techniques

To evaluate the MBE-grown structures, several characterization methods were used. Transmission electron microscopy (TEM), Nomarski, and atomic force microscopy (AFM) techniques were employed to look for defects in the layers and on the surface. Regularity of the lattice and strain from lattice-mismatched growth were examined using x-ray diffraction (XRD) analysis. The Hall effect and van der Pauw method were used to calculate transport properties.

Doping Study Sample Preparation

A study was conducted to determine the effects of doping the AlSb layer on carrier transport and electrical properties. It was expected, based on bulk growth reports, that the AlSb material would exhibit p-type conductivity and that compensation by doping would improve the electrical performance. Doped samples were grown on GaAs substrates using GaTe for n-type and Be for p-type conductivity in the AlSb layer. One undoped AlSb sample and seven doped AlSb samples were compared with an undoped homoepitaxial GaAs sample to rule out contribution from the substrate. Doping with Be ranged from 6×10^{14} cm^{-3} to 1×10^{17} cm^{-3} and with Te from 8×10^9 cm^{-3} to 1×10^{17} cm^{-3}.

For Hall-effect measurements, indium contacts were applied and annealed at 350°C to the corners of cleaved 1 cm × 1 cm samples. Probe tips were pressed into the In contacts to deliver test currents and measure voltage potentials. The sample holder was placed in an electromagnet chamber, where the magnet current was 8.00 A and the field strength was 3.78 kGauss, and triaxial cables were used between the sample and electronics. Two Keithley 617 programmable electrometers, a Keithley 225 programmable current source, a Keithley 7001 switch system, and an HP 34401A multimeter were used to control and measure currents and voltages. A current mirror was developed to reduce the test current from the Keithley 225 when currents smaller than 20 μA were needed. A LabVIEW program was written to coordinate the electronics and calculate mobility, resistivity, and carrier concentration. All Hall measurements were performed at room temperature.

Following the opening of the MBE chamber for cleaning and maintenance, a series of homoepitaxial GaAs samples were grown with decreasing carrier concentration as contaminants were reduced in the chamber. Then, an additional undoped AlSb sample was grown to determine the repeatability of AlSb material quality using MBE methods.

Radiation Detection Experimental Setup

During radiation response measurements, the diode structure was placed with the n-type substrate in contact with a copper plate while probes were placed on the copper plate surface and the p-type side of the structure to deliver bias and to measure output pulses. The microprobe station was kept inside a metal enclosure to reduce radiofrequency (RF) noise. Standard readout electronics were used, and the output signals were converted by Maestro software to produce pulse-height spectra. Sealed radiation sources used included ^{241}Am, ^{252}Cf, and ^{239}Pu, and the distance between the sources and the detector surface was fixed at 10 mm. The thin-film AlSb diodes were cleaved into smaller-area

pieces to improve signal pulse height, per known voltage–capacitance relationships for diodes.

RESULTS AND DISCUSSION

Material Quality Results and Analysis

Growth of AlSb on GaAs substrates introduces a large strain due to the large lattice mismatch (~8%). After a few monolayers of psuedomorphic growth under compression, the epilayer relaxes, leaving an array of periodic dislocations as an interface, as shown in the TEM image in Fig. 1 (left). The threading dislocation density was large near the interface but reduced significantly as the AlSb growth progressed (Fig. 1, right). Nomarski imaging was used to analyze the surface, which was found to be smooth with few defects. The root-mean-square (RMS) roughness was in the range of 1 mm to 2 mm. Screw dislocations (5×10^7 cm^{-2}) were observed with AFM measurements, indicative of shear strain commonly seen with heteroepitaxial growth of antimonides. XRD analysis also showed some strain in the AlSb layer, with full-width at half-maximum (FWHM) of 0.1440°. This corresponds to defect density of 4×10^8 cm^{-2} to 6×10^8 cm^{-2} based on XRD rocking-curve calculations.

Doped AlSb Hall Study Results

The Hall results of the doping study samples are outlined in Table I. The unintentionally doped (UID) GaAs sample, R14-144, measured *p*-type conductivity, as expected, whereas the UID AlSb samples were semi-insulating (SI). With very low Te doping, AlSb samples also exhibited SI behavior, where the carrier type was undetermined due to the very low carrier concentrations measured. As the carrier concentration was reduced, both resistivity and mobility increased, following expectations based on other doped semiconductor material behavior.[9] Measured carrier concentration and dopant cell temperature relations are summed up graphically in the Arrhenius plot in Fig. 2, where the vaporization temperatures were extrapolated to be 295°C and 231°C for Be and Te, respectively. The low-temperature Te-doped samples had lower than intended measured carrier concentration, which may be a result of compensation of immeasurably mildly *p*-type AlSb material.

Comparing theoretical values and bulk results from literature with our epitaxial thin-film results, we show very good resistivity and mobility for undoped AlSb samples. From R14-145, we measured carrier concentration of 2×10^9 cm^{-3}, Hall mobility of 3000 cm^2/V s, and resistivity of 10^6 Ω cm. The sample grown following the MBE chamber maintenance, R15-034, also exhibited high-quality electrical characteristics, with average carrier concentration of 8×10^9 cm^{-3}, average Hall mobility of 900 cm^2/V s, and resistivity of 10^6 Ω cm. This demonstrates reliable growth by MBE for fabricating AlSb devices.

Radiation Detection Results

Direct radiation measurements were performed with the MBE-grown AlSb diodes using ^{252}Cf, ^{241}Am, and ^{239}Pu alpha particles, with calculated fluence rates of 2500 cm^{-2} s^{-1}, 150 cm^{-2} s^{-1}, and 4700 cm^{-2} s^{-1}, respectively, with a portion of the Am alphas blocked by source geometry. For ^{241}Am alpha particles, the detector responses from diode samples with surface areas ranging from 10.5 mm^2 to 1.0 mm^2 are shown in Fig. 3a, where it was observed that detectors with smaller surface area

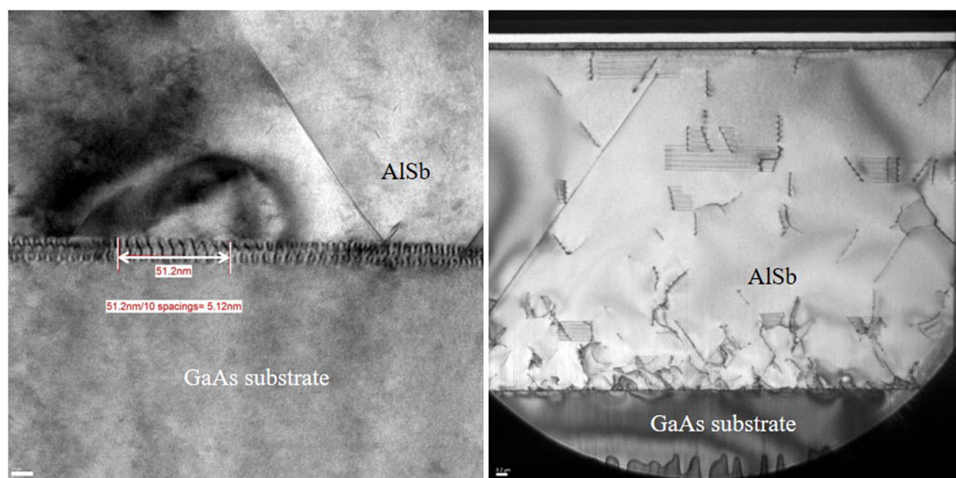

Fig. 1. TEM images of AlSb on GaAs, with higher resolution on left to show lattice dislocation spacing.

Table I. Hall results, ordered by active layer and increasing carrier concentration

Sample	Active layer	Dopant	Dopant cell temperature (°C)	Carrier type	Measured carrier concentration (cm^{-3})	Hall mobility (cm^2/V s)	Resistivity (Ω cm)
R14-144	GaAs	UID	N/A	*p*	5×10^{12}	260	4×10^{3}
R14-145	AlSb	UID	N/A	SI	2×10^{9}	3000	1×10^{6}
R15-034	AlSb	UID	N/A	SI	8×10^{9}	900	1×10^{6}
R14-175	AlSb	Te	320	SI	8×10^{9}	1600	6×10^{5}
R14-178	AlSb	Te	365	SI	2×10^{10}	3000	4×10^{5}
R14-176	AlSb	Be	590	*p*	6×10^{14}	100	1×10^{2}
R14-174	AlSb	Be	615	*p*	1×10^{16}	200	2×10^{0}
R14-172	AlSb	Te	393	*n*	2×10^{16}	60	5×10^{0}
R14-171	AlSb	Be	660	*p*	1×10^{17}	200	2×10^{-1}
R14-177	AlSb	Te	430	*n*	1×10^{17}	140	4×10^{-1}

UID, unintentional doping, i.e., samples with no doping applied.

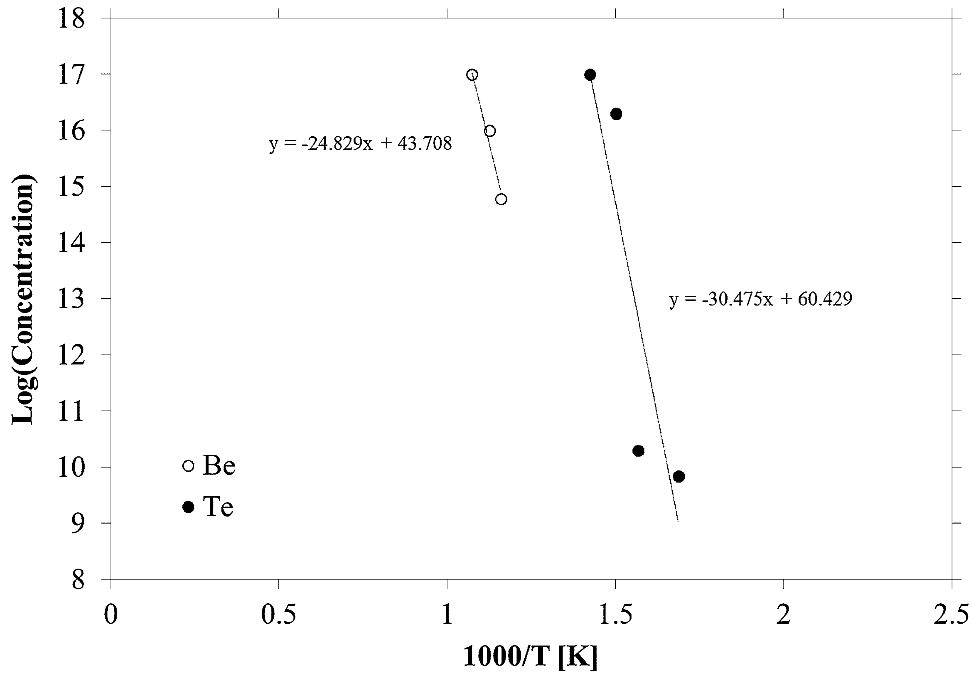

Fig. 2. Arrhenius plot of Te- and Be-doped AlSb samples. Extrapolated vaporization temperatures are 295°C and 231°C for Be and Te dopants, respectively.

produced larger output voltage pulses, associated with higher channel number. This is consistent with capacitance–voltage relationships for diodes, where the diode capacitance increases with the cross-sectional area of the junction[10] and the pulse height is inversely proportional to the capacitance,[11] as seen in other work.[12–14]

As the PIN structure samples were grown prior to optimization studies, the smallest of the diodes (1 mm^2) was used for best signal-to-noise results. The diode *I–V* curve (Fig. 4) is representative of the 1 mm^2 AlSb sample. With more optimized materials based on the current study, diode characteristics and signal to noise are expected to improve greatly. Though full energy was not deposited in the thin active layer, the alpha-particle peaks remained strong and easily discernible above background, and basic energy spectroscopy was performed, comparing the sources over 48 h (Fig. 3b–d). The average centroid for the alpha peaks was channel 135 with standard deviation of 12 channels, resulting in energy resolution of about 9%.

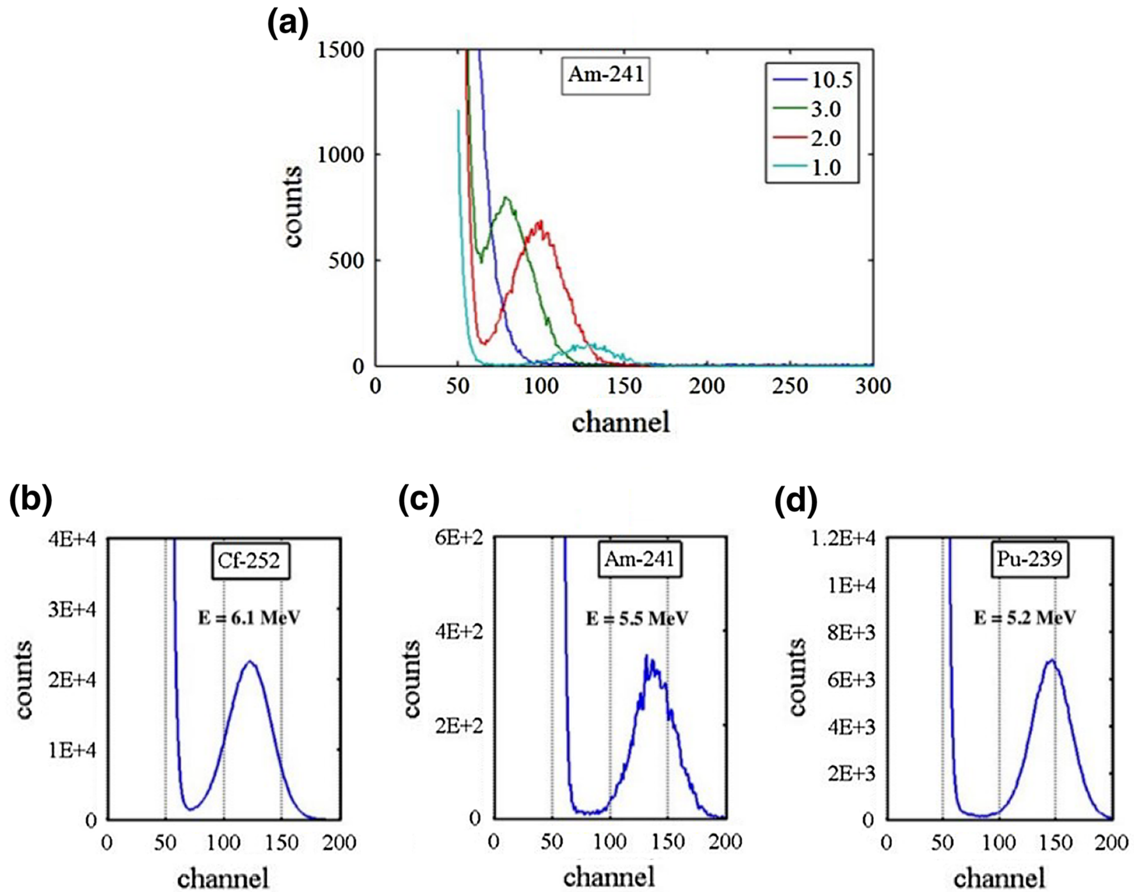

Fig. 3. Radiation response from AlSb room-temperature radiation detectors. (a) Comparison of response for ^{241}Am alpha particles with different diode areas (mm^2), and (b–d) energy spectroscopy with partial energy deposition in the thin detector layer from several alpha-particle sources. The spectra represent approximately 5 mV/channel, or about 700 mV pulse height from the amplifier for the Am peak in the 1.0 mm^2 sample. Stopping power, and thus energy deposited in the thin active layer as the alphas pass through, is lower for higher-energy alphas; full alpha-particle energy is listed for reference.

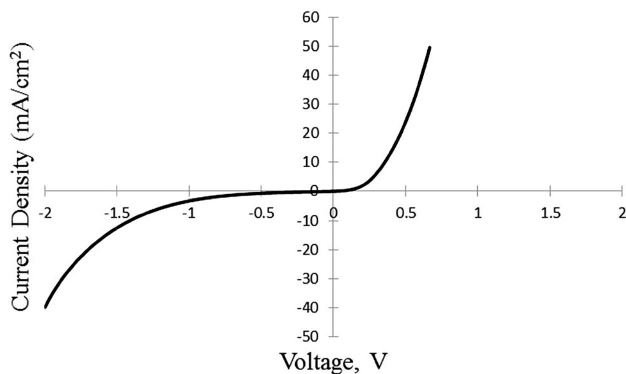

Fig. 4. *I–V* measurement of AlSb PIN diode sample used for radiation detection.

CONCLUSIONS

We demonstrated that detector-grade AlSb devices can be fabricated using UHV MBE methods. High resistivity, high mobility, and low carrier concentrations were achieved without the need for compensation doping. Despite the large lattice mismatch between the substrate and AlSb layers, high-quality material was produced, as evidenced by various characterization results. Additionally, the material quality was consistent and repeatable even when the MBE reactor conditions were not held constant. Improvements to the detector design may be made by using lattice-matched GaSb substrates, which would significantly reduce the number of defects, and/or increasing the AlSb layer thickness, which would allow for larger depletion width and better signal-to-noise response.

ACKNOWLEDGEMENTS

This research was partially supported by the Idaho National Laboratory National Universities Consortium (Contract Number 00044825). The authors would like to thank F. K. Husher for design and construction of the current mirror used for low-current Hall measurements and the microprobe station used for radiation detection measurements.

REFERENCES

1. V.E. Kutny, A.V. Rybka, A.S. Abyzov, L.N. Davydov, V.K. Komar, M.S. Rowland, and C.F. Smith, *Nucl. Instrum. Methods A* 458, 448 (2001).
2. V. Lordi, D. Aberg, P. Erhart, and K.J. Wu, *Proc. SPIE 6706, Hard X-Ray and Gamma-Ray Detector Physics IX,* 67060O (September 21, 2007). doi:10.1117/12.739117.
3. P. Erhart, D. Aberg, B.W. Sturm, K.-J. Wu, and V. Lordi, *Appl. Phys. Lett.* 97, 142104 (2010).
4. S. Subbanna, G. Tuttle, and H. Kroemer, *J. Electron. Mater.* 17, 4 (1988).
5. B. Bennett, W.J. Moore, M.J. Yang, and B.V. Shanabrook, *J. Appl. Phys.* 87, 11 (2000).
6. A. Furukawa and S. Ideshita, *J. Appl. Phys.* 75, 10 (1994).
7. M.D. McCluskey, E.E. Haller, and P. Becla, *Phys. Rev. B* 65, 045201 (2001).
8. M.-H. Du, *Phys. Rev. B* 79, 045207 (2009).
9. D.A. Neamen, *Semiconductor Physics and Devices* (New York, NY: McGraw-Hill, 2003).
10. A. Coche and P. Siffert, *Semiconductor Detectors*, ed. G. Bertolini and A. Coche (Wiley, New York, 1968), p. 107.
11. G. Bertolini, *Semiconductor Detectors*, ed. G. Bertolini and A. Coche (Wiley, New York, 1968), p. 243.
12. R. Steinberg, *A Technique for Increasing the Sensitivity of a Solid-State Fission Probe* (NASA TN D-1054, Washington, 1961).
13. R.T. Klann and D.S. McGregor, *Development of Coated Gallium Arsenide Neutron Detectors* (Baltimore, MD, 2000, ICONE-8110).
14. E.I. Vaughan, N. Rahimi, G. Balakrishnan, and A.A. Hecht, *J. Electron. Mater.* (2015). doi:10.1007/s11664-015-3869-3.